Remote Sensing of Environment 328 (2025) 114878

Contents lists available at ScienceDirect

Remote Sensing of Environment

journal homepage: www.elsevier.com/locate/rse

Monitoring fine-scale natural and logging-related tropical forest degradation using Sentinel-1

Anne-Juul Welsink [a,*], Chloé Dupuis [b], Laura Cue La Rosa [a], Monne Weghorst [c], Jens van der Zee [a], Sietse van der Woude [a], Marielos Peña-Claros [d], Martin Herold [e], Kurt Fesenmyer [f], Johannes Reiche [a]

[a] Laboratory of Geo-Information Science and Remote Sensing, Wageningen University & Research, Droevendaalsesteeg 3, Wageningen, 6708PB, Netherlands
[b] TERRA Teaching and Research Centre, Gembloux Agro-Bio Tech, University of Liege, Passage des Déportés 2, Gembloux, 5030, Belgium
[c] Soil Physics and Land Management Group, Wageningen University & Research, Droevendaalsesteeg 3, Wageningen, 6708PB, Netherlands
[d] Forest Ecology and Forest Management Group, Wageningen University & Research, Droevendaalsesteeg 3, Wageningen, 6708PB, Netherlands
[e] GFZ German Research Centre for Geosciences, Telegrafenberg, Potsdam, 14473, Germany
[f] The Nature Conservancy, 4245 Fairfax Avenue, Suite 100, Arlington, 22203-1606, VA, USA

ARTICLE INFO

Edited by Marie Weiss

Keywords:
Selective logging
Natural disturbance
Radar remote sensing
Forest degradation

ABSTRACT

Tropical forest degradation results in severe biomass loss and biodiversity decline. However, fine-scale natural and logging-related forest disturbances remain difficult to trace, both from the ground as well as remotely. Comprehensive, landscape scale characterization of anthropogenic forest degradation requires accurate accounting of baseline canopy disturbance rates and patterns. This paper has evaluated the feasibility of radar data for detecting canopy gaps created by natural and anthropogenic mechanisms at large spatial scale by assessing the extent to which the Sentinel-1 C-band radar signal can be used to map fine-scale disturbances in both naturally disturbed and logged landscapes. Our physical-based method detects disturbances based on changes in backscatter resulting from radar shadow and/or layover. We apply various detection thresholds to explore the trade-off between detection and false detection and validate our method in study areas for which spatially exhaustive drone-based canopy gap maps are available for validation, namely Barro Colorado Island nature reserve (median gap area: 39 m^2) and five logging concessions in the Congo Basin (median gap area: 237 m^2). With a moderate threshold (2.5 dB backscatter reduction), we reach detection rates above 65 percent for disturbances above 200 m^2 in both naturally disturbed and logged areas. Detection rates were primarily driven by gap area; gap depth had a smaller, yet significant, influence. These results significantly improve on operational forest disturbance products and previous studies on fine-scale disturbance detection using Sentinel-1 radar. Moreover, the improved insight in detection accuracies of anthropogenic disturbances fosters a move towards monitoring forest dynamics across large scales at which we cannot be certain whether the disturbance driver is anthropogenic or natural.

1. Introduction

Our human influence fundamentally alters the Earth's tropical forest biomes, their biodiversity and associated carbon storage (Lewis et al., 2015; Malhi et al., 2014; Weiskopf et al., 2024). This influence is not limited to managed forests. Climate change leads to increased drought-related tree mortality, more frequent and intense wildfires and severe insect outbreaks, among others (Viljur et al., 2022). While the direct impact of large-scale land conversion is evident, fine-scale disturbances can have cascading, indirect effects that result in forest degradation, including the impairment of ecological processes and increasing sensitivity to further forest disturbance (Lapola et al., 2023; Malhi et al., 2014; Pan et al., 2011; Abbas et al., 2020; Vancutsem et al., 2021; Gardner et al., 2009; Bustamante et al., 2016; Assis et al., 2020).

In recent years, several studies have shown that short wavelength (C- and X-band) Synthetic Aperture Radar (SAR) data is a promising data source for fine-scale disturbance detection (Carstairs et al., 2022; Dupuis et al., 2023; Hethcoat et al., 2021; Aquino et al., 2022), thanks to its sensitivity to forest structure, and ability to penetrate clouds (Westman and Paris, 1987; Imhoff, 1995; Evans and Plaut, 1996). Nevertheless, the precise extent of forest degradation remains unclear (Gao et al., 2020), and of 55 countries that have submitted a reference level to the United Nations Framework Convention on

* Corresponding author.
E-mail address: anne-juul.welsink@wur.nl (A.-J. Welsink).

https://doi.org/10.1016/j.rse.2025.114878
Received 7 November 2024; Received in revised form 16 June 2025; Accepted 18 June 2025
Available online 8 July 2025

Climate Change (UNFCCC), only 33 included emissions from degradation (UNFCCC, 2024). Furthermore, European policy such as the Deforestation-free Products Regulation (EUDR) (European Commission, 2023) is largely focused on plantations while ignoring common forestry practices that may cause degradation (Betts et al., 2024).

An important reason for this lack of information is the fact that degradation is difficult to monitor remotely across large areas (Kellner et al., 2009; Kleinschroth et al., 2019; Carstairs et al., 2022; Hethcoat et al., 2021; Welsink et al., 2023). Degradation may be defined as 'a state of anthropogenically induced arrested succession, where ecological processes that underlie forest dynamics are diminished or severely constrained (Ghazoul et al., 2015). Remote sensing methods have a number of – partly inherent – limitations regarding the detection of 'degradation'. First of all, detection systems based on remote sensing cannot distinguish between natural and anthropogenic fine-scale disturbances at the level of individual canopy gaps. Secondly, small gaps or gaps that fall below the canopy are often not visible in remote sensing imagery. Thirdly, it remains challenging to reliably map forest recovery (including the biodiversity value of regrowing vegetation) (Lennox et al., 2018; Heinrich et al., 2023).

Quantifying forest degradation would require an approach in which forest dynamics are monitored over large areas and long term to provide insight in landscape-scale loss, because systematic degradation is too complex to measure at the stand level (Betts et al., 2024). A comprehensive, landscape scale characterization of anthropogenic forest degradation first requires accurate accounting of baseline canopy disturbance rates and patterns. This paper evaluates the feasibility of radar data for detecting canopy gaps created by natural and anthropogenic mechanisms at large spatial scale.

We quantify the potential and limitations of Sentinel-1's C-band radar signal to map for fine-scale disturbances in both natural and anthropogenic disturbance regimes. Previous research has mapped fine-scale forest disturbances at relatively high accuracies, but has remained limited to logging concessions (Aquino et al., 2022; Carstairs et al., 2022; Dupuis et al., 2023). Natural disturbances have frequently been excluded from monitoring efforts due to a lack of reference data. However, with tree mortality rates ranging from 1.88 percent to 3.38 percent per year (Anon, 2004), natural disturbance dynamics have a strong influence on above-ground carbon storage (Galbraith et al., 2013; Johnson et al., 2016). To move towards monitoring forest dynamics across large scales – at which we cannot be certain whether the disturbance driver is anthropogenic or natural – we require information on the detection accuracy of both fine-scale anthropogenic and natural disturbances.

We focus on reference areas in both naturally disturbed and logged landscapes for which spatially exhaustive canopy gap maps were available for validation (Cushman et al., 2022; Dupuis et al., 2023), namely the strictly protected Barro Colorado Island (BCI) nature reserve in Panama and five different logging concessions across the Congo Basin. We consider 'fine-scale disturbances' as present in the reference datasets, with a mean gap area of 245 m^2.

Natural and logging-related disturbances typically differ in typical gap area and depth and these factors are likely to influence detection. While natural gaps are typically shallow and small, logging-related gaps tend to nearly reach the ground, where the tree was felled (Zuleta et al., 2023; Simonetti et al., 2023). It is generally problematic to determine whether remotely sensed fine-scale disturbances have a 'natural' or human-induced cause (Stahl et al., 2023). In this study, we used a reference dataset from BCI, one of the most studied tropical forests worldwide. The island has been administered by the Smithsonian since 1946 and since 1923, no logging or tree extraction has occurred. Therefore, we may assume that observed disturbances in this reference area have a natural cause (Anon, 2004).

We produced fine-scale forest disturbance maps for our reference areas using Sentinel-1 time series using a physically-based approach, which makes use of radar shadow and layover effects that result from the influence of canopy gaps on the side-looking radar signal. We tested various detection thresholds to understand the trade-off between detection and false detection. Secondly, we assessed detection of disturbances in relation to gap characteristics, such as size and depth. Thirdly, we compared the use of radar shadow, layover, and both combined for gap detection. No previous study that we know of has quantified the added value of layover for gap detection. Finally, we show how detection using the presented method compares to the radar shadow based detection systems by Carstairs et al. (2022) and Dupuis et al. (2023) and two state-of-the-art forest change products, namely the GFW's integrated alerts (Reiche et al., 2024) and the European Commission's Joint Research Centre (JRC)'s TMF product (Vancutsem et al., 2021).

2. Materials and methods

2.1. Sentinel-1 data

We used Sentinel-1 C-band (5.6 cm) Ground Range Detected (GRD) data in Interferometric Wide Swath Mode (IW), which has a resolution of 20 × 22 m and 10 m pixel spacing (Potin et al., 2016), covering the tropics every 12 days by an ascending or descending orbit. The radar signal is emitted from a side-looking geometry at an 'incidence' angle between 29.1 and 46 degrees. This side-looking geometry results in radar shadow, which can be used to identify canopy gaps, as demonstrated by existing research (Reiche et al., 2021; Carstairs et al., 2022; Bouvet et al., 2018). Radar shadow occurs where canopy gaps prevent most signal return, resulting in low backscatter values (Fig. 1). The remaining tree line at the far range of a canopy gap (farthest away from the sensor) results in relatively high backscatter. This is spread over a larger area as a result of the layover effect. The strength of shadow and layover is further influenced by the density of the forest canopy, which determines to what extent the signal can penetrate (van der Woude et al., 2024). We used data from the dominant orbit direction (ascending or descending) for each study area, because the direction of the side-looking satellite has an influence on the relative location of shadow and layover.

The size of shadow and layover depends on the incidence angle, as well as on gap width and depth (Fig. 1). Shadow length = $\tan(\alpha) \times$ gap depth, where (α) is the incidence angle. Layover length = $\tan(90° - \alpha) \times$ tree height. With a canopy height of 30 m, this results in a shadow size between 16.7 and 31.1 m and a layover size between 29.0 and 53.9 m, depending on the incidence angle. A larger incidence angle results in an increase in shadow and a decrease in layover, although in most instances the layover will be larger than the shadow. The pixel spacing of Sentinel-1 in a regular grid usually does not align exactly with the occurrence of shadow and layover, resulting in mixed pixels. Often, shadow and layover effects are spread over multiple pixels, indicating potential disturbance in an area larger than that of the actual disturbance. In other cases, mixed pixels obscure the signal to the extent that shadow and layover are barely visible. Therefore, detected disturbances are not necessarily in proportion to the size of the actual disturbances on the ground.

2.2. Reference data

We used two separate datasets for validation in naturally disturbed and logged landscapes (Fig. 2). On BCI, Panama, we used a dataset of natural disturbances between 2018 and 2020 (Cushman et al., 2022). In line with Cushman et al. (2022), we assume that the disturbances on BCI will have a natural cause.

Drone flights in June–July of 2018 and 2020 allowed Cushman et al. (2022) to calculate two canopy height models. The authors define a disturbance as a decrease in canopy height larger than 5 m over an area of at least 25 m^2, provided that the initial canopy height was at least 10 m. The dataset excludes areas within 25 m from the coast,

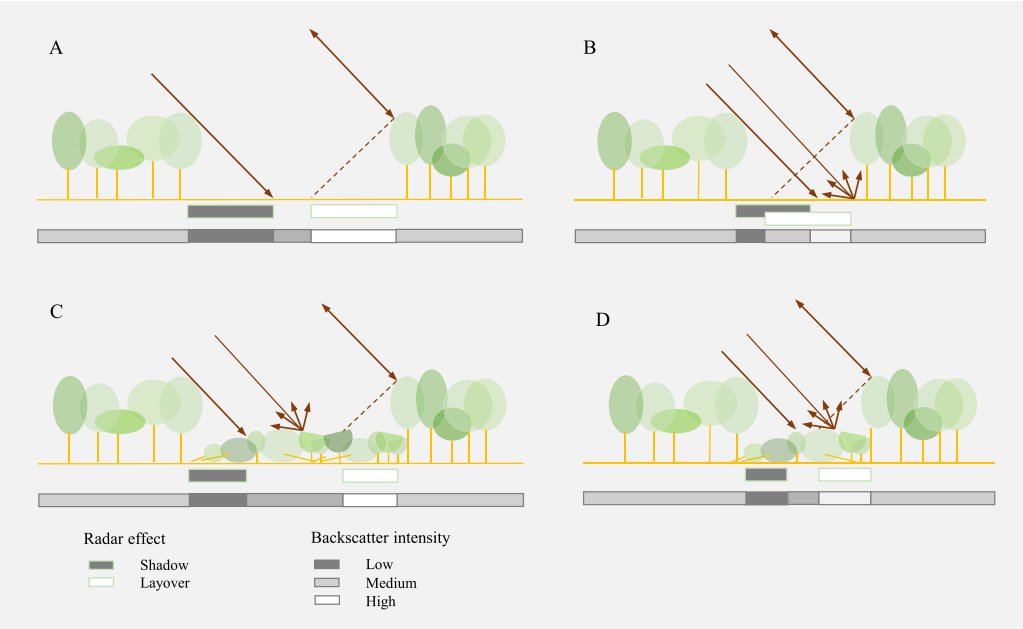

Fig. 1. Schematic representation of the size and strength of radar shadow and layover in relation to gap width and depth. A-B and C-D represent a decrease in gap width, while A-C and B-D represent a decrease in gap depth. Radar shadow and layover are outlined in green, the resulting backscatter in grey.

buildings, actively maintained clearings, and areas with inadequate drone imagery. The majority of gaps had an area below 100 m^2 (Fig. 3). Disturbance area and gap depth were positively related.

For validation of logging-related disturbances, we used a dataset of canopy gaps in five FSC-certified concessions across Cameroon, Gabon, and the Republic of the Congo, ranging between 5 and 33 km^2 in size. Each of these concessions was exploited in different years between 2018 and 2021 (Dupuis et al., 2023; Dupuis, 2024) (Supplement Appendix A.2). Drone flights covered the concessions before and after logging in Gabon and the Republic of Congo, and after logging in Cameroon. Based on the resulting orthomosaics and digital surface models, gaps were manually delineated based on visual interpretation, distinguishing between felling gaps, skid trails, roads, log yards, and unidentified drivers. Note that the last category may include a limited proportion of natural disturbances, provided that they are visible in the drone data and were not filtered out by the repeated drone flights. While skid trails are generally linear features, only the parts visible in drone data were included in the reference dataset. As a result, skid trails in the reference dataset are characterized by relatively small, disconnected disturbances. We excluded roads from the reference dataset, because FSC-certified logging companies are required to establish roads at least one year before logging advances to allow the soil to compact and dry. Therefore, roads should not trigger disturbance detections during the monitoring period. The reference dataset for the Congo Basin does not include data on gap depth, but logging gaps generally reach close to the ground, where the log was removed.

The distribution of gap area includes a relatively high proportion of smaller gaps across the reference areas in both the BCI and the Congo Basin, although the average gap area was higher for logging-related disturbances than for natural gaps (Fig. 3). The mean gap area for natural gaps was 113 m^2 and the median 39 m^2. The mean area of disturbances larger than 900 m^2 was 2115 m^2. Logging-related disturbances had a mean area of 387 m^2 and a median of 237 m^2. Disturbances larger than 900 m^2 had a mean area of 1675 m^2.

2.3. Disturbance detection

The following section details how we created Sentinel-1 change composites, which served as the basis for disturbance detection. Next, we introduce various thresholds and requirements to define which pixels qualify as disturbances according to our methods.

2.3.1. Change composites

Change composites mitigate the effect of speckle or moisture variations on the Sentinel-1 signal. They represent the change in pixel values during a trailing 3 month monitoring period in relation to a trailing 2 year historical period (change ratio pixel i = mean pixel value historical period - mean pixel value monitoring period). We assigned the date of the middle month of the monitoring period to each change composite. A buffer of 4 months between the historical and monitoring period limits the representation of disturbance signals in both.

2.3.2. Defining disturbance thresholds

An undisturbed forest canopy results in low change ratios, with change composite pixel values around 0 in both VV and VH radar polarization (Fig. 4). Negative VV and VH ratios may suggest a disturbance if it exceeds the signal to noise ratio. Positive values may imply direct backscatter, layover, or double bounce (although the latter will not be present in very fine-scale canopy gaps). Because layover is a characteristic signal related to forest disturbances (Fig. 1), it could potentially facilitate detection of fine-scale disturbances. We tested detection based on shadow, layover, and both combined. Since radar layover did not contribute positively to the detection, all further analyses were based on solely radar shadow. We also tested classifying pixels as disturbed when either VV or VH exceeded the radius threshold, rather than both. However, the results were not included in this paper because they did not prove promising.

We applied various thresholds to determine how large the increase or decrease in backscatter should be to indicate disturbance. We used a circle equation for this purpose: $r^2 = (VV)^2 + (VH)^2$, where VV and VH refer to the change composite signal in dB. We varied r between 1 and 4 in steps of 0.5 to assess the effect on the detection performance. Higher thresholds will result in relatively conservative detection.

Pixels were classified as disturbed if they met the criteria for at least 3 consecutive months. Forest disturbances will result in a change in the three-dimensional forest structure that remains visible for at least a number of months, before potential regrowth. Therefore, if the pixel value criteria are met for multiple consecutive months, we can be rather

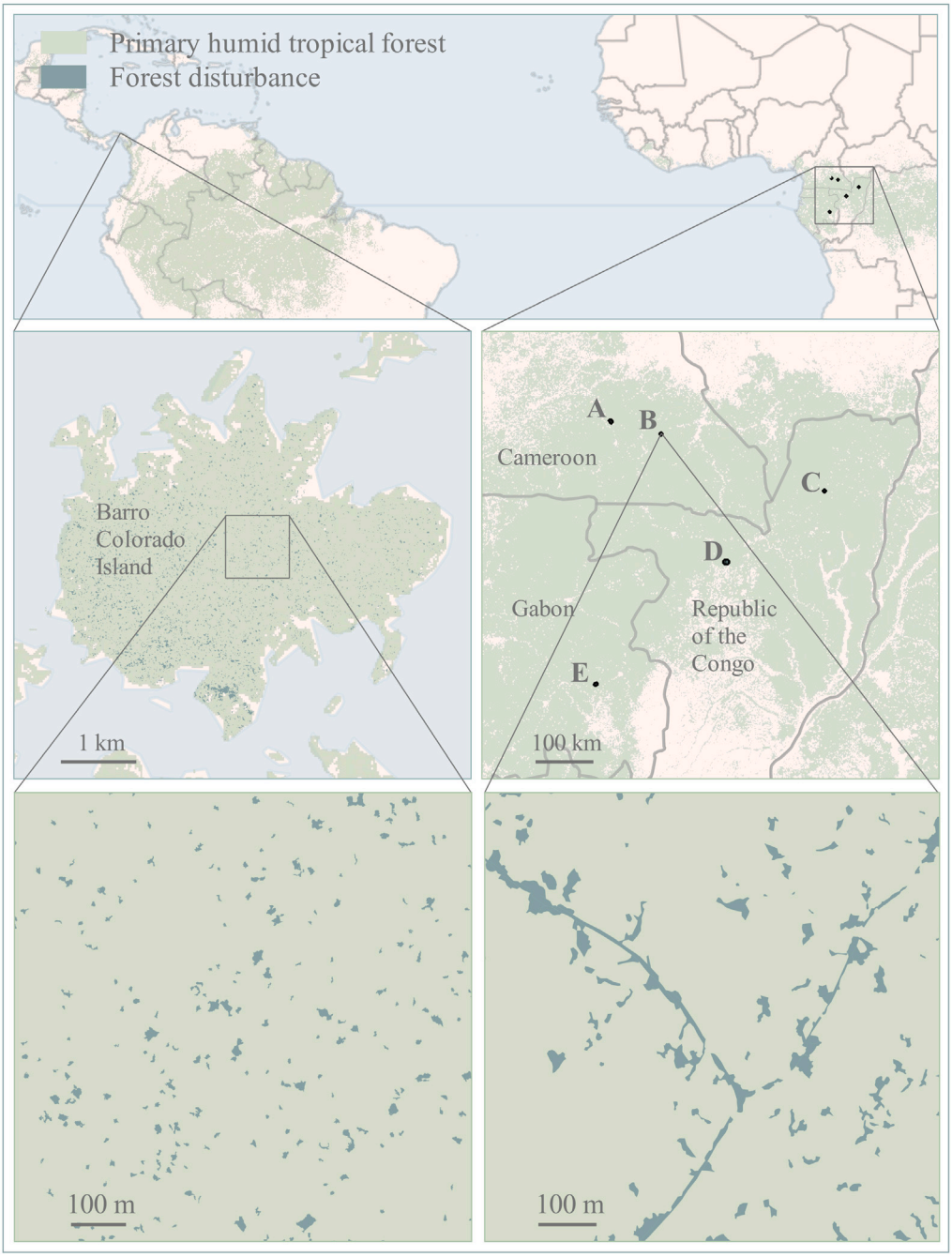

Fig. 2. Overview map of the study areas, with natural disturbances in Barro Colorado Island and logging-related disturbances in five concessions in the Congo Basin.

certain that the forest was indeed disturbed (For a comparison of detection rates using 1–5 consecutive months, see Supplement Appendix A.3).

We present results for various minimum mapping units (a criterion for the minimum number of connected pixels for something to be classified as a disturbance) based on 8-connectedness. If only a single pixel suits the above criteria, the chance is higher that this is noise than when multiple connected pixels do so (Reiche et al., 2021; Hirschmugl et al., 2020; Bouvet et al., 2018). In addition, we performed a logistic regression to test to what extent detection was driven by gap area. For the BCI, we also assessed the impact of gap depth.

2.4. Validation

The following section introduces the time periods for which we mapped forest disturbances in each reference area, presents the event-based validation procedure and explains how we compared our results with state-of-the-art forest change products.

2.4.1. Time periods for disturbance mapping

The temporal characteristics of the reference datasets in the Congo Basin and the BCI were different. Therefore, we used a different set-up in both areas to obtain mapped disturbances from an appropriate period for comparison.

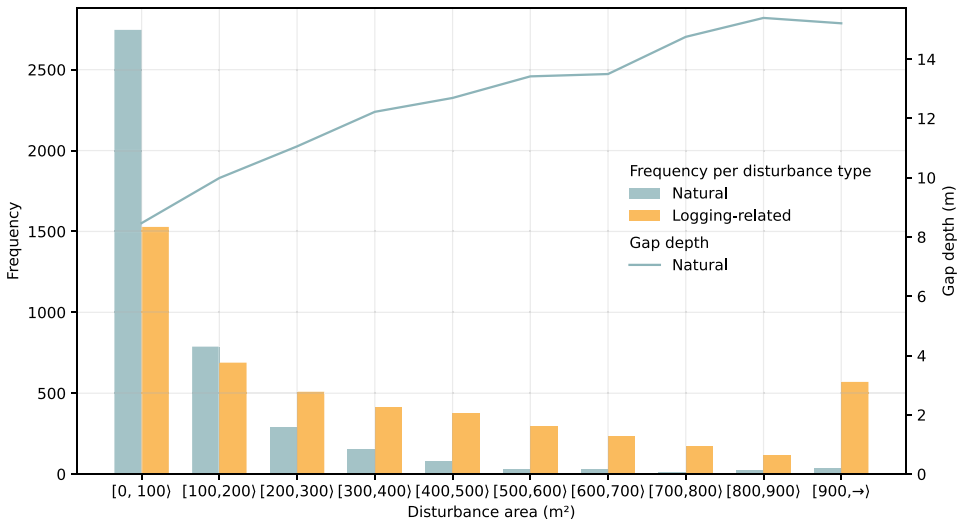

Fig. 3. Size distribution of natural disturbances on Barro Colorado Island and logging-related disturbances in the Congo Basin and average gap depth of natural disturbances per size category.

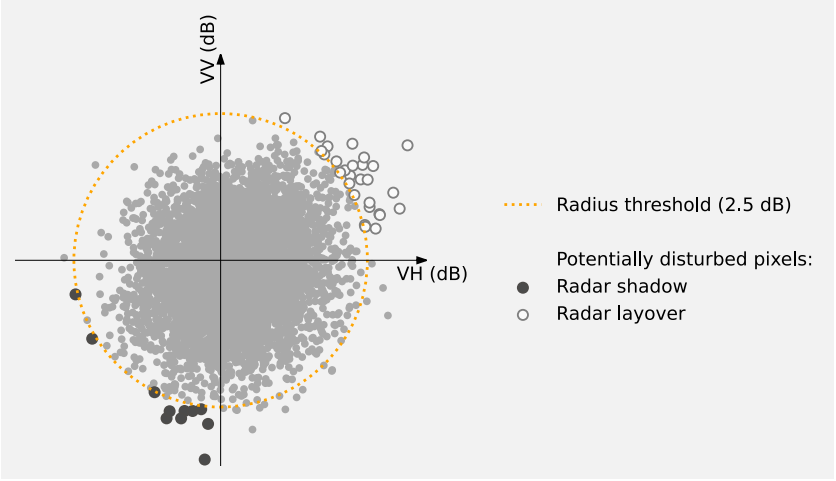

Fig. 4. Example of radius threshold of 2.5 dB applied to a random sample of 5000 pixel values in a single change composite. Pixel values should indicate shadow or layover in three consecutive change composites to be classified as disturbance.

For the BCI study area, we mapped disturbances for the period from June 2018 until August 2020, exactly capturing the period for which disturbances were included in the reference dataset (Fig. 5).

For the study area in the Congo Basin, we mapped disturbances for the year each concession was harvested, with 4 months before and 7 months after the reported month of logging (Fig. 5). This temporal buffer allowed us to capture any early or late logging instances, as well as delayed detections. Inclusion of this temporal buffer is possible because the disturbance period in a logging concession is controlled, i.e. we know the approximate start and end period of harvest, and we know that there was no harvest activity before or after this period.

In both study areas, we ran the detection system for a period of 4 additional months before the start of the monitoring period, and then removed the detections from these dates (Fig. 5). This cut-off period prevents disturbances that occurred in earlier months (such as roads that were established in advance of harvesting activities) from being wrongly labelled with a date early in the monitoring period.

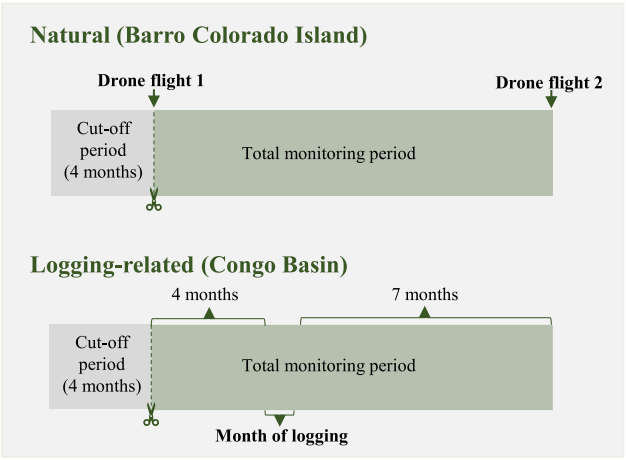

Fig. 5. Time periods of disturbance mapping in relation to reference data acquisition for natural disturbances in Barro Colorado Island and reported harvest for logging-related disturbances in the Congo Basin.

2.4.2. Event-based validation

We performed a map comparison for validation in which we related our mapped detections to disturbance events as captured by the exhaustive, spatially explicit reference maps. In such an event-based

validation, a disturbance is considered correctly detected as soon as it is partly identified, as opposed to a pixel-based validation in which the overlap between pixels is used to measure the level of agreement between mapped disturbances and the reference dataset (Tang et al., 2019). An event-based approach was preferable over a pixel-based validation, which is sensitive to misalignment between the mapped disturbances and the reference data (Congalton and Green, 2019).

We used the following calculations to obtain the detection rate (1 - omission error) and false detection rate (commission error):

$$\text{Detection rate} = \frac{\text{N correct detections}}{\text{N correct detections} + \text{N omissions}}, \quad (1)$$

$$\text{False detection rate} = \frac{\text{N commissions}}{\text{N commissions} + \text{N correct detections}}. \quad (2)$$

The *filterBounds* function was used in Google Earth Engine to assess the intersection of mapped and actual disturbances. No minimum surface percentage of overlap was applied. For an overview of the overlap between disturbances and their corresponding mapped detections, (see Appendix A.4). We calculated the detection rate and false detection rate separately for various gap area categories. The size category of correct detections and omissions was derived from the area of gaps in the reference data, while the size of commissions was derived from the mapped disturbances. We also calculated the detection rate and false detection rate for various gap depths for the BCI study area, and for various disturbance types for the Congo Basin.

2.4.3. Comparison with state-of-the-art forest change products

We compared detection of disturbances using the presented methodology to detection using the radar shadow based detection system by Carstairs et al. (2022) the machine learning algorithm by Dupuis et al. (2023) and two state-of-the-art forest change products (Vancutsem et al., 2021; Reiche et al., 2024). Carstairs et al. (2022) use a similar logic to ours, in which they compare VV and VH values of a historical period to the mean pixel values during a monitoring period. However, while our detections are based on a circle equation, they use the function VV * VH + 0.64(VV + VH) > 0, where both VV and VH < 0 (see Appendix A.1 for a visual example). We compared our results to their detections for the same time periods, based on the version of their algorithm as published with the publication via Google Earth Engine. Carstairs et al. (2022) do not use a buffer between their historical period and monitoring period. Furthermore, for a pixel to classify as a disturbance, we require three consecutive months above the radius threshold, while Carstairs et al. (2022) require the average change ratio over 25 Sentinel-1 observations (close to 10 months) to fall below their threshold function.

Dupuis et al. (2023) used Sentinel-1 radar imagery in a machine learning algorithm trained on an extensive dataset of more than 6000 geo-referenced harvest gaps to map disturbances in a single forest concession in Cameroon. Similar to our method, the authors used a time-series approach comparing backscatter values during a (12-months) historical window to those during the 3 months following disturbance. Dupuis et al. (2023) apply a minimum mapping unit of 500 m^2. We compare our results with their mapped disturbances for the only concession for which they are available (Concession A in Fig. 2).

The first forest change product that we used for comparison is the integrated GFW alerts system, which combines the optical Global Analysis and Discovery (GLAD)-Sentinel-2 and GLAD-Landsat alerts with the Sentinel-1 based RAdar for Detecting Deforestation (RADD) alerts with at a minimum mapping unit of 5 pixels (Reiche et al., 2024). In our study areas, there was no coverage from Sentinel-2 during the period of interest, so the detections of the integrated alerts were solely based on Sentinel-1 and Landsat. We used integrated GFW alerts from the same time period as the detection system presented in this paper and used the reference datasets on BCI and the Congo Basin for validation.

Secondly, we used the TMF product from the JRC for comparison (Vancutsem et al., 2021). This is an annual product which aims at capturing changes in tropical moist forest cover based on 30 m resolution Landsat data. Even if a calendar year was only partly covered by our disturbance maps, we included disturbances from that year as captured by the annual TMF product. The detection rate using the TMF product for both the BCI and the Congo Basin will therefore have a slight positive bias.

3. Results

3.1. Effect of radius thresholds, gap area, and gap depth

Radius thresholds determine the balance between detection and false detection (Fig. 6). The lower the radius threshold, the higher both the detection and false detection rate. The false detection rate remained relatively high across size categories for the three least conservative thresholds (1, 1.5 and 2). This is true for both natural disturbances on BCI and logging-related disturbances in the Congo Basin.

The detection of disturbances was strongly driven by gap area for both natural disturbances on BCI and logging-related ones in the Congo Basin (Fig. 6), as confirmed by the logistic regression results (Supplement Appendix A.6.1). On BCI, the detection rate was particularly low for smaller disturbances, which are particularly prevalent in the naturally disturbed BCI, as visible in an example area (Fig. 7). The low detection rate of the smallest disturbances persisted even with less conservative radius thresholds. The false detection rate decreased quickly once an alert area of 200 m^2 was reached.

Next to disturbance size, gap depth also had a significant influence, based on the data from BCI (Fig. 8, supplement Appendix A.6.1). The deeper the gap, the higher the detection rate. Furthermore, there is a strong correlation between gap depth and gap area, as reflected by the limited number of observations above 500 m^2 for the shallowest gap depth category.

3.2. Use of radar shadow and layover

Inclusion of layover in the detection system in addition to radar shadow provides a slight increase in the detection rate for each threshold compared to shadow only (Fig. 9). However, this comes at the cost of an increase in the false detection rate, especially for higher radius thresholds. Detection using just layover results in the lowest overall detection rates, and the highest false detection rates across all thresholds for both natural and logging-related disturbances.

3.3. Comparison with state-of-the-art forest change products

The presented method based on radar shadow and a radius threshold of 2.5 dB resulted in a significant improvement in disturbance detection compared to existing monitoring systems, such as the integrated GFW alerts and the TMF product, as well as the map by Dupuis et al. (2023) (Fig. 10). Detection rates were similar across concessions, although the false detection rate was relatively high in concession A (Supplement Appendix A.5). The method by Carstairs et al. (2022) reached a similar detection rate to our algorithm, but has a higher false detection rate, especially for natural disturbances on BCI.

4. Discussion

4.1. Effect of radius thresholds, gap area, and gap depth

Gap characteristics such as gap area and depth have a significant influence on the Sentinel-1 signal, both in theory and practice. In line with our theoretical expectation based on the properties of Sentinel-1 (Fig. 1), shallower and smaller gaps are relatively difficult to detect. Gaps below 200 m^2 were relatively poorly detected and had a relatively

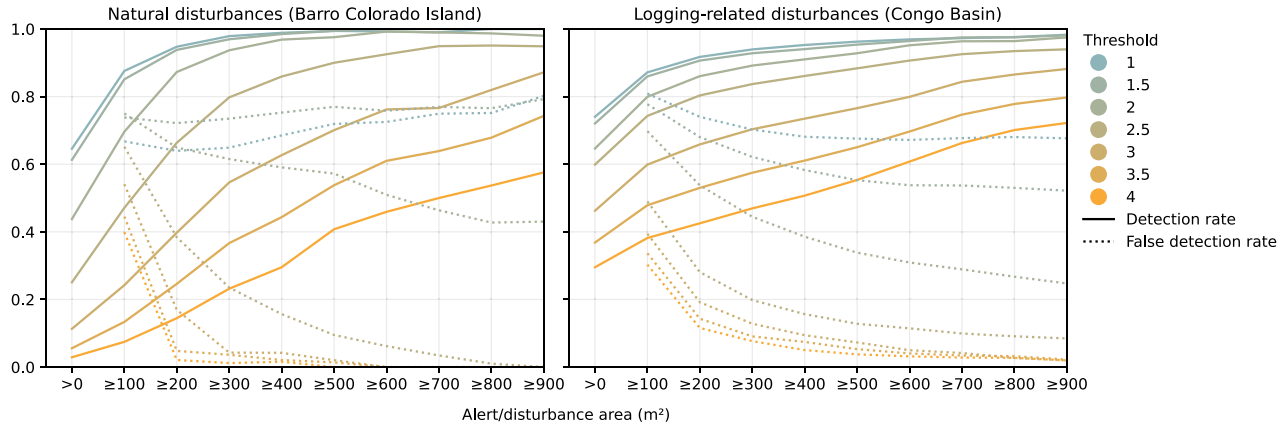

Fig. 6. Detection rate and false detection rate for different radius thresholds for natural disturbances on Barro Colorado Island and logging-related ones in the Congo Basin (based on just radar shadow).

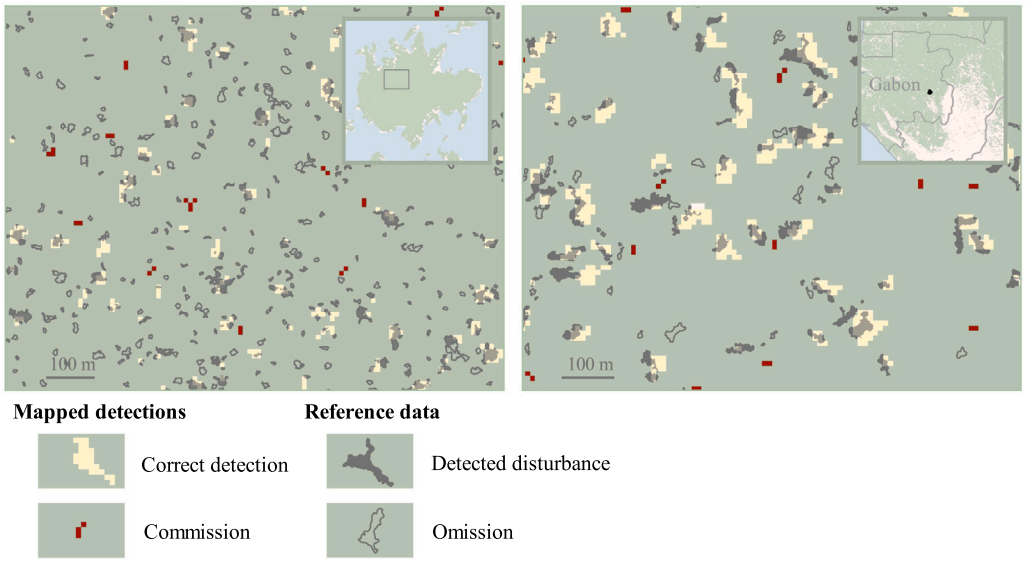

Fig. 7. Example of mapped disturbances (radius threshold 2.5 dB) and reference data for natural disturbances in Barro Colorado Island (Centre coordinate: −79.85035,9.15774) and logging-related disturbances in the Congo Basin (Centre coordinate: 13.29333,−0.82537). Note that we used an event-based validation, where detections are considered correct once they intersect with an actual disturbance, even when they are offset.

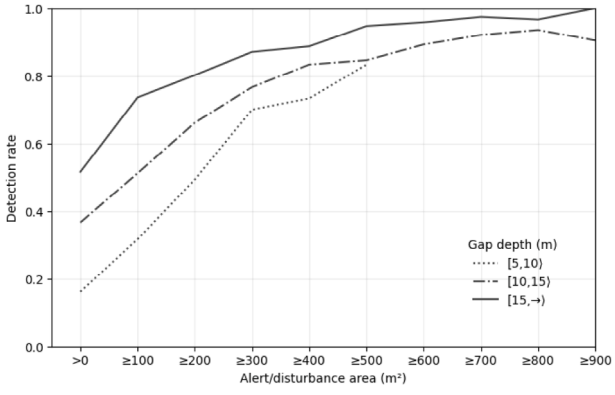

Fig. 8. Detection rate for different gap depth classes and disturbance sizes for natural disturbances in Barro Colorado Island (radius threshold 2.5 dB). Categories with less than 5 observations were excluded (this was the case for gaps with a depth between 5 and 10 m and an area above 600 m^2 in size.).

high false detection rate across all thresholds. This is in line with the Sentinel-1-based study by Carstairs et al. (2022), who excluded any gaps below 200 m^2 from their analysis. The smallest gaps are relatively difficult to detect because they are more likely to be obscured as a result of mixed pixels. At the same time, false detections are likely to be small because the chance that several 'noisy' pixels are connected is small. In few cases, commission errors may be related to missed disturbances in the reference data, which are more likely to be small as well.

The influence of gap area and depth provides an important part of the explanation as to why the detection rates were higher for logging-related disturbances in the Congo Basin compared to natural disturbances on BCI (Fig. 3). While logging-related disturbances tend to be larger and deeper as they often imply the removal of one or more entire trees (combined with frequent collateral damage), natural disturbances tend to be smaller and shallower as they often include branch falling and dead standing trees (Simonetti et al., 2023; Zuleta et al., 2023). Differences in (false) detection rates may also be related to forest structure, where BCI has relatively open forest with more roughness, while concessions in the Congo Basin tend to have a more continuous canopy. However, this influence will be less pronounced than the influence of gap size and depth, considering the limited

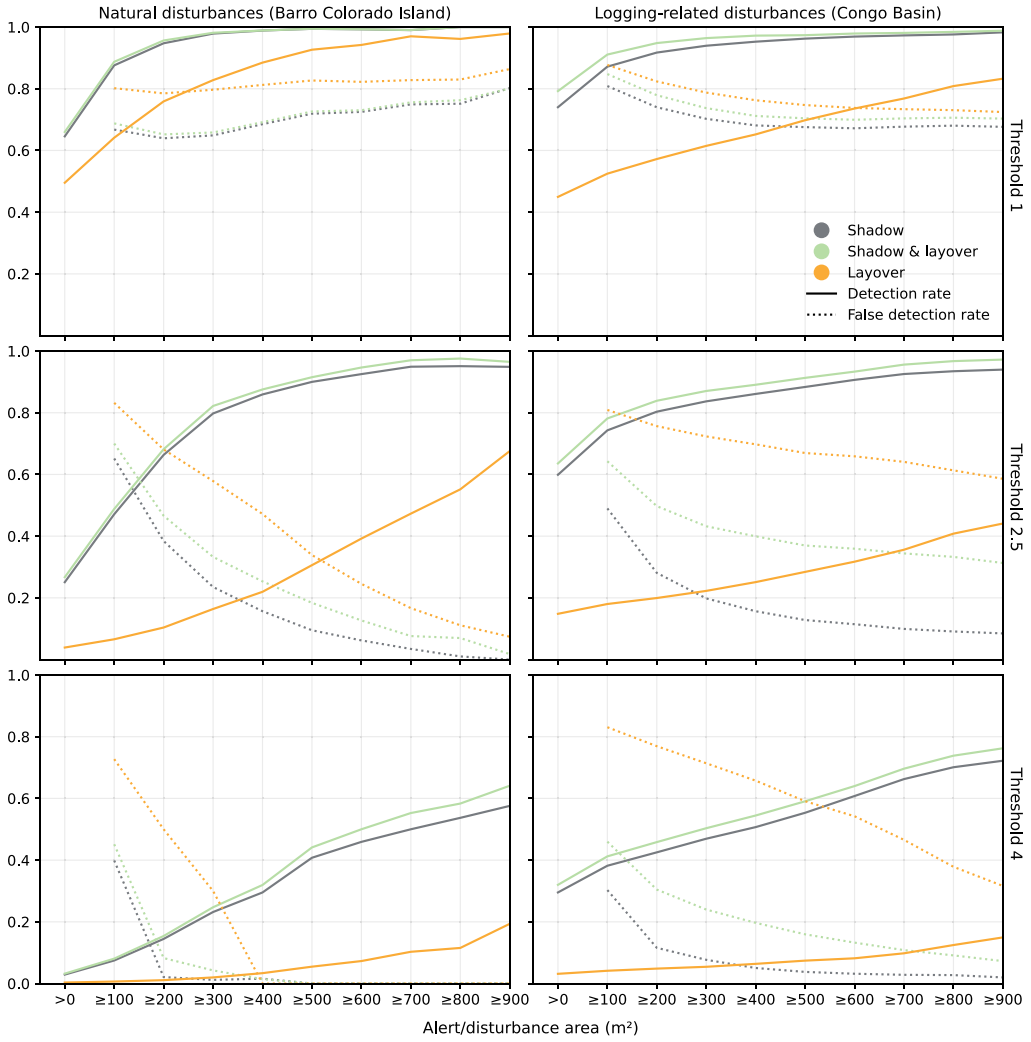

Fig. 9. Detection rate and false detection rate for detection based on radar shadow, layover, or both combined for natural disturbances (Barro Colorado Island) and logging-related ones (Congo Basin), comparing radius thresholds of 1 dB, 2.5 dB, and 4 dB.

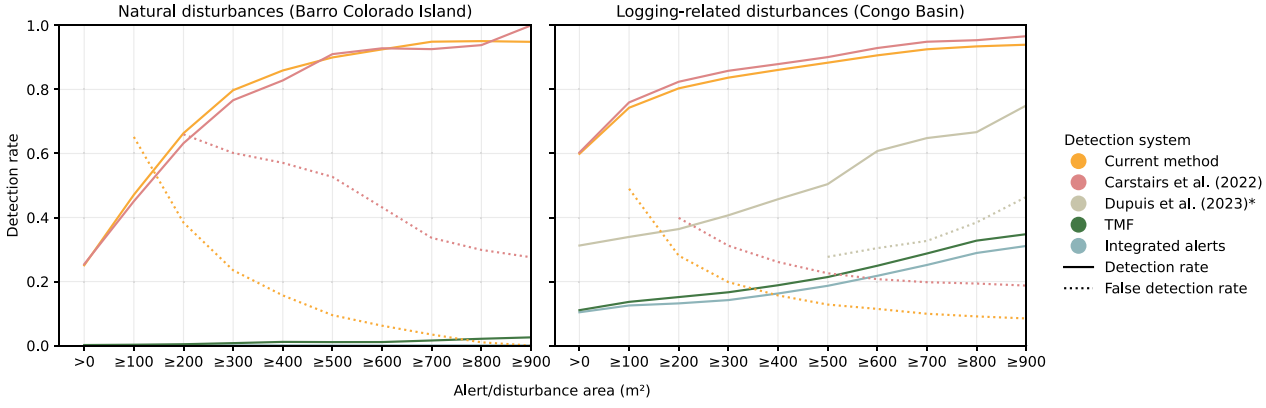

Fig. 10. Comparison of detection systems for natural disturbances in Barro Colorado Island and logging-related disturbances in the Congo Basin. Detection using the current method was based on radar shadow with a radius threshold of 2.5 dB. False detection rates are only shown for the current method, Carstairs et al. (2022) and Dupuis et al. (2023), because the minimum mapping unit of the TMF product and the GFW integrated alerts makes this statistic unsuitable for small size categories. Carstairs et al. (2022) and Dupuis et al. (2023) apply a minimum mapping unit of 200 m^2 and 200 m^2, respectively, so they do not find false detections below those sizes. *Detections by Dupuis et al. (2023) were only available for one concession (concession A).

differences in detection rates across logging concessions in spite of differences in forest types (Supplement Appendix A.2, Appendix A.5).

A trade-off between detection and false detection rates is inherent to many (remote sensing) detection systems (Craiu and Sun, 2008), and is also evident in the assessment of disturbance detection using various thresholds. We suggest using a threshold of 2.5 for a relatively high detection rate while limiting the increase in false detections. However, the cost of incomplete detection versus false detection may differ across

use cases. Our explicit representation of this trade-off provides users with the opportunity to make an informed decision regarding the desired balance between detection and false detection for their specific needs (Fig. 6).

4.2. Use of radar shadow and layover

Radar layover did not prove very suitable for disturbance detection. This can be explained by the fact that the layover signal is relatively weak because it is mixed with the signal returned from remaining canopy structure (Fig. 1). The drop in detection rate resulting from an increase of the radius threshold from 1 to 2.5 dB was much larger with detection based on just layover than for detection based on shadow or shadow and layover combined (Fig. 9). This was in line with expectations, because an increase in threshold will impact a relatively weak (mixed) signal more than a stronger shadow signal. This effect is less apparent when the radius threshold is raised even further, which results in a significant decrease in the detection rate using just shadow.

Furthermore, with thresholds above 2.5 dB, the increase in accuracy gets larger as disturbance size increases for layover, while the increase in accuracy decreases with disturbance size for radar shadow. Smaller disturbances tend to show limited layover (Fig. 1), so layover does not contribute much to their detection. With a radius threshold of 1 dB, the increase in accuracy decreases with disturbance size (Fig. 9). This is likely because the threshold is so lenient that it includes noise, as confirmed by the high false detection rate.

4.3. Comparison with state-of-the-art forest change products

The results from the current study confirm that Sentinel-1 can be used to detect logging-related and natural disturbances. Both physical-based approaches by Carstairs et al. (2022) and this study based on radar shadow performed better than the machine learning based approach by Dupuis et al. (2023). An added benefit of these physical-based approaches is the fact that they are relatively easily transferable to different areas when new reference data becomes available for testing, while the machine learning approach of Dupuis et al. (2023) was trained specifically on logging gaps in a single forest type. Using a conservative radius threshold of 2.5 dB, we reached similar accuracies on individual gap detection as Carstairs et al. (2022), but with lower false detection rate, especially for detection of natural disturbances. The fact that we require a shorter period to confirm a disturbance (4 months in total, as opposed to almost 10 months for Carstairs et al., 2022) is an added benefit for monitoring purposes that require somewhat-near-real-time data.

The distribution of VV and VH values of detected disturbances and false detections provides insight in the differences in detection and false detection rates between our current method and Carstairs et al. (2022). The distribution of pixel values of detected disturbances shows a relatively even spread around VV = VH (Fig. 11). Carstairs et al. (2022) detect a relatively high number of disturbances near the area where VV = VH which our current method misses (red samples in Fig. 11), while we detect disturbances that Carstairs et al. (2022) miss where VV or VH is relatively high (yellow samples). The relatively high density of disturbances in the area that we omit explains why Carstairs et al. (2022) reach a slightly higher detection rate for logging related disturbances than to our method. However, the false detections show a similar spread of VV and VH values compared to correctly detected disturbances. As a result, setting lower thresholds in any part of the negative VV-VH-plane will lead to an increase in the detection rate, but also an increase in the false detection rate. This suggests that both Carstairs et al. (2022) and our current method are close to an optimized detection algorithm when using single pixel Sentinel-1 backscatter data, where our method has a somewhat lower false detection rate. Further improvement (e.g. by combining our rulesets) is unlikely to generate a higher detection rate without an increase in false detection. Therefore, efforts to further improve fine-scale disturbance detection will likely benefit from inclusion of different sensors.

Our method detected a much higher percentage of disturbances than commonly used state-of-the-art forest change products such as the TMF product and the integrated GFW alerts (Reiche et al., 2024; Vancutsem et al., 2021). While these systems reach high detection accuracies on larger forest disturbances (Reiche et al., 2024), they respectively detected 4 and 10 percent of all the fine-scale disturbances in our logged reference dataset and less than 1 percent in the naturally disturbed BCI (Fig. 10).

Similar to the method presented in this paper, the integrated GFW alerts and the TMF product gained slightly higher accuracies on the logging-related disturbances in the Congo Basin compared to the natural disturbances on BCI (Fig. 10). As shown in this paper, gap area and depth will have an influence on radar detection. However, these factors will also influence detection based on optical imagery, which provides the basis for the TMF product and the optical data used in the integrated GFW alerts (next to Sentinel-1 data). Disturbances are particularly difficult to detect based on optical imagery if the soil is not visible, which is common for the relatively shallow natural gaps. Even in the drone orthomosaics from Cushman et al. (2022), disturbances on BCI could often not be visually identified, let alone in Sentinel-2 or Landsat. The relatively low resolution of the Landsat data on which the TMF product is based explains the limited detection of fine-scale disturbances. Moreover, the 5 pixel minimum mapping unit of the integrated GFW alerts filters fine-scale disturbances out even if they are detected.

Recently, Bourgoin et al. (2024) have quantified the extent of human degradation, comparing GEDI measurements of forest structure in different classes of forest cover change ('degraded', 'intact', and near forest edges), as derived from the TMF product. The authors conclude that human degradation is greater than previously estimated, but this research was based on the TMF product which only captures a fraction of the forest degradation as measured by our reference datasets (Fig. 10). The TMF product was particularly poor at detecting the smaller and shallower disturbances in our datasets (Fig. 10), which implies that it tends to capture mostly high intensity disturbances. Future research could complement the work by Bourgoin et al. (2024) by analysing canopy structure changes in more fine-scale disturbances, aided by GEDI as well as upcoming data streams such as and NISAR L-band radar time series.

4.4. Limitations

4.4.1. This study

While disturbances above 200 m^2 were detected relatively well in both naturally disturbed and logged landscapes, the majority of canopy gaps in both reference datasets was below 200 m^2 (87 percent on BCI, and 55 percent in the Congo Basin). This implies that we only capture part of the spectrum of natural and human-made disturbances. Furthermore, Simonetti et al. (2023) have shown that around 17 percent of the tree-mortality and fallen branches are likely not observed from the top of the canopy. Such below-canopy disturbances were not included in the drone-based reference data, and will also not be detected by current high-resolution satellite remote-sensing based alert systems. Similarly, our system may be challenged by tree mortality events that result in only a partial change in canopy structure, such as insect or disease outbreak or collateral logging damage that slowly kills trees leaving them defoliated but still with branches and trunks (Shenkin et al., 2015).

Some technical characteristics of the Sentinel-1 signal also require attention. First of all, we want to highlight again that the size of actual disturbances and their shadow in Sentinel-1 does not exactly correspond (Fig. 7). Mapped disturbances are often larger and sometimes smaller than their counterparts in the real world. At the same

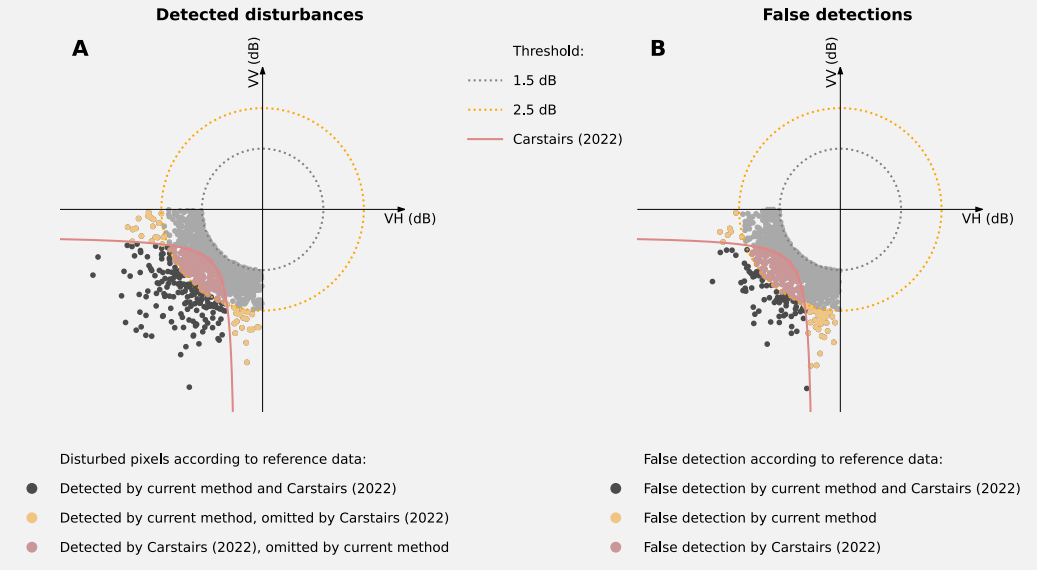

Fig. 11. Comparison of the (dotted yellow) radius function used for detection in the current method and the (solid red) function used by Carstairs et al. (2022), namely VV * VH + 0.64(VV + VH) > 0, where both VV and VH < 0. We used a radius threshold of 1.5 dB to generate a random sample of 1000 pixels values of (A) detected disturbances (pixel-based) and (B) false detections. Based on this sample, we show which pixels would be detected with a threshold of 2.5 dB and using the function from Carstairs et al. (2022). The distribution of pixel values explains differences in (false) detection rates between the presented method (yellow + black) and the function used by Carstairs et al. (2022) (red + black).

time, mixed pixels blur the radar signal, which contributes to the limited detection of especially the smallest disturbances. Furthermore, some limitations in the reference datasets need to be considered. First of all, the reference datasets did not allow for detailed validation of the temporal accuracy of the presented method. Such validation would be an important prerequisite for future research on fine-scale disturbance dynamics over time. Secondly, the dataset on BCI only included gaps that were at least 25 m^2 and 5 m deep. It remains unclear how frequently Sentinel-1 picks up on gaps that are shallower and/or smaller. Furthermore, the two-year interval between drone flights may have been long enough for some (particularly small and/or shallow) disturbances to regrow, excluding them from the reference canopy height change models. This could imply that some commission errors were actually correctly captured disturbances, but would also cover up some missed detections.

The dataset in the Congo Basin was based on visual delineation of gaps. Although targeted towards logging-related disturbances, it may include some natural disturbances inside of logging concessions. However, visual identification of natural gaps based on optical data is particularly challenging as these generally do not reach the ground. This suggests that both on BCI and in the Congo Basin, part of the false detections may be related to actual disturbances which were not included in the reference datasets (Fig. 11). Future research should try to understand the origin of false detections, and to what extent they are related to limitations in the reference data.

While detection rates were relatively similar across concessions, one concession had relatively many false detections (Supplement Appendix A.5). This concession contains various wetlands. Moisture has a strong effect on the radar signal, and water bodies provide a particularly low backscatter. Areas changing from relatively dry to wetter are therefore easily mistaken for disturbances due to the drop in backscatter. Future research should take backscatter signal fluctuations in such wetlands into account and adapt detection methods accordingly.

4.5. Implications for monitoring degradation & forest dynamics

Forest degradation will be a focal point in future commitments towards environmental conservation (Silva Junior et al., 2021). The consistent availability of free Sentinel-1 time series provides great opportunity to monitor the spatio-temporal distribution of disturbances across the tropics, and the presented methodology offers potential for monitoring in both natural and logged landscapes.

This insight in detection accuracies of both natural and anthropogenic disturbances opens up opportunities towards monitoring forest dynamics across large scales at which we cannot be certain of the disturbance driver. This will allow for improved landscape-level degradation monitoring (Betts et al., 2024). Importantly, the resilience of tropical forest biomes is further affected by unprecedented stress from climate change (Wang et al., 2024), which drives forest ecosystems towards critical tipping points and potential collapse (Flores et al., 2024). Insight in disturbance patterns across landscapes could support forest conservation by improving our understanding of the impact of climate change on forest dynamics, forest structure and vulnerability to climate extremes (Bauman et al., 2022; McDowell et al., 2020; Lyra et al., 2017; Viljur et al., 2022; Brinck et al., 2017).

Furthermore, improved fine-scale disturbance monitoring will support forest management and certification, as well as the enforcement of policies such as Forest Law Enforcement Governance and Trade (FLEGT) and the EUDR (European Commission, 2003, 2023) to move beyond its current focus on plantation forestry (Betts et al., 2024). Analyses of the spatio-temporal configuration of disturbances in logging concessions could provide insight into harvest intensities (Bénédet et al., 2024; Maurent et al., 2023). Moreover, disturbance intensity could be studied in relation to management practices at small scales (e.g. annual harvesting compartments), rather than only at the concession level, as demonstrated by Ellis et al. (2019) based on field data from various harvest blocks.

Improved fine-scale disturbance monitoring will provide a stepping stone for a more accurate estimation of emissions and mitigation potential from natural as well as logging-related disturbances (Griscom et al., 2017). This is particularly promising at aggregated levels, considering the limited relationship between gap area and alert size, and high uncertainty as to whether a gap is related to a single tree fall or includes collateral damage. However, this requires spatially explicit and exhaustive reference data on emissions from natural disturbances, logging and other drivers of degradation, which is scarce (Ellis et al., 2019).

In spite of increasing opportunities, monitoring efforts should acknowledge that only certain disturbance drivers and sizes can be detected remotely (Thompson et al., 2013). For example, tree mortality rates are generally relatively high for smaller trees (Gora and Esquivel-Muelbert, 2021), fire frequently affects only the understory (depending on its intensity and recurrence) (Slik and Eichhorn, 2003), and while biotic drivers such as drought, wind, and lightning tend to have a relatively large effect on large trees, dead standing trees can be difficult to detect as well (Gora and Esquivel-Muelbert, 2021; Yanoviak et al., 2020; Bennett et al., 2015).

Finally, improved fine-scale disturbance monitoring opens up the opportunity to evaluate patterns of disturbance relative to ancillary data such as land tenure, distance from forest edges and the type of management (e.g. comparing industrial logging concessions and community managed forest areas). This could enhance our understanding of mechanisms of degradation. Nevertheless, caution is required, because as advancements in remote sensing allow us to monitor increasingly fine-scale disturbances beyond industrial logging concessions, the risk emerges that cultural practices of local and Indigenous communities are driven illegal (Wells et al., 2022). While most concessions in Central Africa are predominantly large scale, it is crucial that the importance of tree harvesting for people's livelihoods is acknowledged and considered in the context of forest monitoring, because forests cannot be conserved without considering the livelihoods of the people living off it.

5. Conclusion

To move towards monitoring forest dynamics across large scales at which we cannot be certain whether the disturbance driver is anthropogenic or natural, information is required on the detection accuracy of natural disturbances. Previous studied have reached high accuracies on detection of fine-scale disturbances in logging concessions (Carstairs et al., 2022; Dupuis et al., 2023). This paper has assessed to what extent the Sentinel-1 C-band radar signal can be used to map fine-scale disturbances in both naturally disturbed and logged landscapes. We validated our physical based detection method based on changes in backscatter resulting from radar shadow and/or layover using spatially exhaustive drone-based canopy gap maps in Barro Colorado Island nature reserve and five logging concessions in the Congo Basin. We compared the results to the operational integrated GFW alerts, the TMF product and two existing Sentinel-1 based methods which were not previously validated on natural disturbances (Carstairs et al., 2022; Dupuis et al., 2023).

Our detection method reached significantly higher accuracies compared to the integrated GFW alerts, the TMF product and machine learning based approach by Dupuis et al. (2023). The physical based study using Sentinel-1 radar shadow by Carstairs et al. (2022) reached similar detection rates, but our false detection rate is more than 10 percent point lower for anthropogenic disturbances and more than 25 percent point lower for natural disturbances across gap sizes. Detection were primarily driven by gap area; gap depth had a smaller, yet significant, influence. The benefit of layover for disturbance detection was not previously quantified in a published study, but proved limited. By quantifying improving (false) detection rates of fine-scale disturbances across naturally disturbed and logged landscapes, this study contributes towards comprehensive, landscape scale characterization of anthropogenic forest degradation, which requires accurate accounting of baseline canopy disturbance rates and patterns.

6. Data accessibility

Reference data for the BCI is publicly available via the Smithsonian institute. Reference data for the Congo Basin is available upon reasonable request. The GFW integrated alerts are available from the GFW website. JRC's TMF product is available from https://forobs.jrc.ec.europa.eu/the EU science hub and on Google Earth Engine. This work contains modified Copernicus Sentinel-1 data (2016-2021), which is available through the Sentinel Hub and on Google Earth Engine. Code to detect fine-scale forest disturbances is openly available via Google Earth Engine.

CRediT authorship contribution statement

Anne-Juul Welsink: Writing – review & editing, Writing – original draft, Visualization, Validation, Methodology, Formal analysis, Data curation, Conceptualization. **Chloé Dupuis:** Writing – review & editing, Data curation. **Laura Cue La Rosa:** Writing – review & editing, Conceptualization. **Monne Weghorst:** Writing – review & editing, Visualization, Validation. **Jens van der Zee:** Writing – review & editing, Methodology. **Sietse van der Woude:** Writing – review & editing, Conceptualization. **Marielos Peña-Claros:** Writing – review & editing, Supervision. **Martin Herold:** Writing – review & editing, Supervision, Funding acquisition. **Kurt Fesenmyer:** Writing – review & editing, Conceptualization. **Johannes Reiche:** Writing – review & editing, Supervision, Project administration, Methodology, Funding acquisition, Conceptualization.

Declaration of competing interest

The authors declare that they have no known competing financial interests or personal relationships that could have appeared to influence the work reported in this paper.

Acknowledgements

The authors would like to thank Ethan Belair and Peter Ellis from The Nature Conservancy and Bart Slagter from Wageningen University for inspiring discussions and thoughtful questions. We would like to thank the two anonymous peer reviewers for their time, effort, and excellent suggestions.

A.W. received funding from the European Space Agency (ESA) Earth Observation for Sustainable Development (EO4SD) initiative (ESA ESRIN/Contract No. 4000131862/20/I-DT). A.W. and J.R. received funding from Norway's Climate and Forest Initiative (NICFI); the US Government's SilvaCarbon program; L.C.R and J.R. received funding from the Open Domain Science project Forest Carbon Crime (Project Number: OCENW.M.21.203) of the Nederlandse Organisatie voor Wetenschappelijk Onderzoek (NWO). S.W. and J.R. received funding from the Open-Earth-Monitor Cyberinfrastructure project (grant agreement No. 101059548) and The ForestWard Observatory to Secure Resilience of European Forests (FORWARDS) project (grant agreement No. 101084481). M.P.C. was supported by Apasia Grant 015.014.006. M.H. was supported by the CGIAR MITIGATE+ project. K.F. was supported by the Bezos Earth Fund.

Appendix A. Supplementary data

Supplementary material related to this article can be found online at https://doi.org/10.1016/j.rse.2025.114878.

Data availability

Data will be made available on request.

References

Abbas, S., Wong, M.S., Wu, J., Shahzad, N., Muhammad Irteza, S., 2020. Approaches of satellite remote sensing for the assessment of above-ground biomass across tropical forests: Pan-tropical to national scales. Remote. Sens. 12 (20), 3351.

Anon, 2004. Tropical Forest Diversity and Dynamism: Findings from a Large-Scale Plot Network. University of Chicago Press, Chicago, IL, p. 459,

Aquino, C., Mitchard, E.T., McNicol, I.M., Carstairs, H., Burt, A., Puma Vilca, B.L., Obiang Ebanéga, M., Modinga Dikongo, A., Dassi, C., Mayta, S., et al., 2022. Reliably mapping low-intensity forest disturbance using satellite radar data. Front. For. Glob. Chang. 5, 1018762.

Assis, T.O., De Aguiar, A.P.D., Von Randow, C., de Paula Gomes, D.M., Kury, J.N., Ometto, J.P.H., Nobre, C.A., 2020. CO2 emissions from forest degradation in Brazilian Amazon. Environ. Res. Lett. 15 (10), 104035.

Bauman, D., Fortunel, C., Delhaye, G., Malhi, Y., Cernusak, L.A., Bentley, L.P., Rifai, S.W., Aguirre-Gutiérrez, J., Menor, I.O., Phillips, O.L., et al., 2022. Tropical tree mortality has increased with rising atmospheric water stress. Nature 608 (7923), 528–533.

Bénédet, F., Gourlet-Fleury, S., Allah-Barem, F., Baya, F., Beina, D., Cornu, G., Dimanche, L., Dubiez, É., Forni, É., Freycon, V., et al., 2024. 40 years of forest dynamics and tree demography in an intact tropical forest at M'Baïki in central Africa. Sci. Data 11 (1), 734.

Bennett, A.C., McDowell, N.G., Allen, C.D., Anderson-Teixeira, K.J., 2015. Larger trees suffer most during drought in forests worldwide. Nat. Plants 1 (10), 1–5.

Betts, M.G., Yang, Z., Hadley, A.S., Hightower, J., Hua, F., Lindenmayer, D., Seo, E., Healey, S.P., 2024. Quantifying forest degradation requires a long-term, landscape-scale approach. Nat. Ecol. Evol. 8 (6), 1054–1057.

Bourgoin, C., Ceccherini, G., Girardello, M., Vancutsem, C., Avitabile, V., Beck, P., Beuchle, R., Blanc, L., Duveiller, G., Migliavacca, M., et al., 2024. Human degradation of tropical moist forests is greater than previously estimated. Nature 1–7.

Bouvet, A., Mermoz, S., Ballère, M., Koleck, T., Le Toan, T., 2018. Use of the SAR shadowing effect for deforestation detection with sentinel-1 time series. Remote. Sens. 10 (8), 1250.

Brinck, K., Fischer, R., Groeneveld, J., Lehmann, S., Dantas De Paula, M., Pütz, S., Sexton, J.O., Song, D., Huth, A., 2017. High resolution analysis of tropical forest fragmentation and its impact on the global carbon cycle. Nat. Commun. 8 (1), 14855.

Bustamante, M.M., Roitman, I., Aide, T.M., Alencar, A., Anderson, L.O., Aragão, L., Asner, G.P., Barlow, J., Berenguer, E., Chambers, J., et al., 2016. Toward an integrated monitoring framework to assess the effects of tropical forest degradation and recovery on carbon stocks and biodiversity. Global Change Biol. 22 (1), 92–109.

Carstairs, H., Mitchard, E.T., McNicol, I., Aquino, C., Chezeaux, E., Ebanega, M.O., Dikongo, A.M., Disney, M., 2022. Sentinel-1 shadows used to quantify canopy loss from selective logging in gabon. Remote. Sens. 14 (17), 4233.

Congalton, R.G., Green, K., 2019. Assessing the Accuracy of Remotely Sensed Data: Principles and Practices. CRC Press.

Craiu, R.V., Sun, L., 2008. Choosing the lesser evil: trade-off between false discovery rate and non-discovery rate. Statist. Sinica 861–879.

Cushman, K., Detto, M., García, M., Muller-Landau, H.C., 2022. Soils and topography control natural disturbance rates and thereby forest structure in a lowland tropical landscape. Ecol. Lett. 25 (5), 1126–1138.

Dupuis, C., 2024. Monitoring Canopy Disturbances in Central Africa: From the Ground to the Sky (Ph.D. thesis). ULiège. GxABT - Liège Université. Gembloux Agro-Bio Tech, ORBi-University of Liège.

Dupuis, C., Fayolle, A., Bastin, J.F., Latte, N., Lejeune, P., 2023. Monitoring selective logging intensities in central Africa with sentinel-1: A canopy disturbance experiment. Remote Sens. Environ. 298, 113828.

Ellis, P.W., Gopalakrishna, T., Goodman, R.C., Putz, F.E., Roopsind, A., Umunay, P.M., Zalman, J., Ellis, E.A., Mo, K., Gregoire, T.G., et al., 2019. Reduced-impact logging for climate change mitigation (RIL-c) can halve selective logging emissions from tropical forests. Forest Ecol. Manag. 438, 255–266.

European Commission, 2003. Communication from the Commission to the Council and the European Parliament - Forest Law Enforcement, Governance and Trade (FLEGT) - Proposal for an EU Action Plan. Eur-Lex, URL https://eur-lex.europa.eu/legal-content/EN/TXT/?uri=CELEX:52003DC0251.

European Commission, 2023. Regulation (EU) 2023/1115 of the European Parliament and of the Council of 31 May 2023 on the making available on the Union market and the export from the Union of certain commodities and products associated with deforestation and forest degradation and repealing Regulation (EU) No 995/2010. Eur-Lex, URL https://eur-lex.europa.eu/legal-content/EN/TXT/?uri=CELEX:32023R1115&qid=1687867231461.

Evans, D.L., Plaut, J.J., 1996. Science Results from the Spaceborne Imaging Radar-C/X-Band Synthetic Aperture Radar (SIR-C/X-SAR): Progress Report. Technical Report, National Aeronautics and Space Administration.

Flores, B.M., Montoya, E., Sakschewski, B., Nascimento, N., Staal, A., Betts, R.A., Levis, C., Lapola, D.M., Esquível-Muelbert, A., Jakovac, C., et al., 2024. Critical transitions in the Amazon forest system. Nature 626 (7999), 555–564.

Galbraith, D., Malhi, Y., Affum-Baffoe, K., Castanho, A.D., Doughty, C.E., Fisher, R.A., Lewis, S.L., Peh, K.S.-H., Phillips, O.L., Quesada, C.A., et al., 2013. Residence times of woody biomass in tropical forests. Plant Ecol. Divers. 6 (1), 139–157.

Gao, Y., Skutsch, M., Paneque-Gálvez, J., Ghilardi, A., 2020. Remote sensing of forest degradation: a review. Environ. Res. Lett. 15 (10), 103001.

Gardner, T.A., Barlow, J., Chazdon, R., Ewers, R.M., Harvey, C.A., Peres, C.A., Sodhi, N.S., 2009. Prospects for tropical forest biodiversity in a human-modified world. Ecol. Lett. 12 (6), 561–582.

Ghazoul, J., Burivalova, Z., Garcia-Ulloa, J., King, L.A., 2015. Conceptualizing forest degradation. Trends Ecol. Evolut. 30 (10), 622–632.

Gora, E.M., Esquivel-Muelbert, A., 2021. Implications of size-dependent tree mortality for tropical forest carbon dynamics. Nat. Plants 7 (4), 384–391.

Griscom, B.W., Adams, J., Ellis, P.W., Houghton, R.A., Lomax, G., Miteva, D.A., Schlesinger, W.H., Shoch, D., Siikamäki, J.V., Smith, P., et al., 2017. Natural climate solutions. Proc. Natl. Acad. Sci. 114 (44), 11645–11650.

Heinrich, V.H., Vancutsem, C., Dalagnol, R., Rosan, T.M., Fawcett, D., Silva-Junior, C.H., Cassol, H.L., Achard, F., Jucker, T., Silva, C.A., et al., 2023. The carbon sink of secondary and degraded humid tropical forests. Nature 615 (7952), 436–442.

Hethcoat, M.G., Carreiras, J.M., Edwards, D.P., Bryant, R.G., Quegan, S., 2021. Detecting tropical selective logging with C-band SAR data may require a time series approach. Remote Sens. Environ. 259, 112411.

Hirschmugl, M., Deutscher, J., Sobe, C., Bouvet, A., Mermoz, S., Schardt, M., 2020. Use of SAR and optical time series for tropical forest disturbance mapping. Remote. Sens. 12 (4), 727.

Imhoff, M.L., 1995. A theoretical analysis of the effect of forest structure on synthetic aperture radar backscatter and the remote sensing of biomass. IEEE Trans. Geosci. Remote Sens. 33 (2), 341–351.

Johnson, M.O., Galbraith, D., Gloor, M., De Deurwaerder, H., Guimberteau, M., Rammig, A., Thonicke, K., Verbeeck, H., Von Randow, C., Monteagudo, A., et al., 2016. Variation in stem mortality rates determines patterns of above-ground biomass in A mazonian forests: implications for dynamic global vegetation models. Global Change Biol. 22 (12), 3996–4013.

Kellner, J.R., Clark, D.B., Hubbell, S.P., 2009. Pervasive canopy dynamics produce short-term stability in a tropical rain forest landscape. Ecol. Lett. 12 (2), 155–164.

Kleinschroth, F., Laporte, N., Laurance, W.F., Goetz, S.J., Ghazoul, J., 2019. Road expansion and persistence in forests of the Congo Basin. Nat. Sustain. 2 (7), 628–634.

Lapola, D.M., Pinho, P., Barlow, J., Aragão, L.E., Berenguer, E., Carmenta, R., Liddy, H.M., Seixas, H., Silva, C.V., Silva-Junior, C.H., et al., 2023. The drivers and impacts of Amazon forest degradation. Science 379 (6630), eabp8622.

Lennox, G.D., Gardner, T.A., Thomson, J.R., Ferreira, J., Berenguer, E., Lees, A.C., Mac Nally, R., Aragão, L.E., Ferraz, S.F., Louzada, J., et al., 2018. Second rate or a second chance? Assessing biomass and biodiversity recovery in regenerating Amazonian forests. Global Change Biol. 24 (12), 5680–5694.

Lewis, S.L., Edwards, D.P., Galbraith, D., 2015. Increasing human dominance of tropical forests. Science 349 (6250), 827–832.

Lyra, A., Imbach, P., Rodriguez, D., Chou, S.C., Georgiou, S., Garofolo, L., 2017. Projections of climate change impacts on central America tropical rainforest. Clim. Change 141, 93–105.

Malhi, Y., Gardner, T.A., Goldsmith, G.R., Silman, M.R., Zelazowski, P., 2014. Tropical forests in the Anthropocene. Annu. Rev. Environ. Resour. 39 (1), 125–159.

Maurent, E., Hérault, B., Piponiot, C., Derroire, G., Delgado, D., Finegan, B., Kientz, M.A., Amani, B.H., Bieng, M.A.N., 2023. A common framework to model recovery in disturbed tropical forests. Ecol. Model. 483, 110418.

McDowell, N.G., Allen, C.D., Anderson-Teixeira, K., Aukema, B.H., Bond-Lamberty, B., Chini, L., Clark, J.S., Dietze, M., Grossiord, C., Hanbury-Brown, A., et al., 2020. Pervasive shifts in forest dynamics in a changing world. Science 368 (6494), eaaz9463.

Pan, Y., Birdsey, R.A., Fang, J., Houghton, R., Kauppi, P.E., Kurz, W.A., Phillips, O.L., Shvidenko, A., Lewis, S.L., Canadell, J.G., et al., 2011. A large and persistent carbon sink in the world's forests. Science 333 (6045), 988–993.

Potin, P., Rosich, B., Grimont, P., Miranda, N., Shurmer, I., O'Connell, A., Torres, R., Krassenburg, M., 2016. Sentinel-1 mission status. In: Proceedings of EUSAR 2016: 11th European Conference on Synthetic Aperture Radar. VDE, pp. 1–6.

Reiche, J., Balling, J., Pickens, A.H., Masolele, R.N., Berger, A., Weisse, M.J., Mannarino, D., Gou, Y., Slagter, B., Donchyts, G., et al., 2024. Integrating satellite-based forest disturbance alerts improves detection timeliness and confidence. Environ. Res. Lett. 19 (5), 054011.

Reiche, J., Mullissa, A., Slagter, B., Gou, Y., Tsendbazar, N.-E., Odongo-Braun, C., Vollrath, A., Weisse, M.J., Stolle, F., Pickens, A., et al., 2021. Forest disturbance alerts for the congo basin using Sentinel-1. Environ. Res. Lett. 16 (2), 024005.

Shenkin, A., Bolker, B., Peña-Claros, M., Licona, J.C., Putz, F.E., 2015. Fates of trees damaged by logging in Amazonian Bolivia. Forest Ecol. Manag. 357, 50–59.

Silva Junior, C.H., Carvalho, N.S., Pessôa, A.C., Reis, J.B., Pontes-Lopes, A., Doblas, J., Heinrich, V., Campanharo, W., Alencar, A., Silva, C., et al., 2021. Amazonian forest degradation must be incorporated into the COP26 agenda. Nat. Geosci. 14 (9), 634–635.

Simonetti, A., Araujo, R.F., Celes, C.H.S., da Silva e Silva, F.R., dos Santos, J., Higuchi, N., Trumbore, S., Marra, D.M., 2023. Gap geometry, seasonality and associated losses of biomass–combining UAV imagery and field data from a Central Amazon forest. Biogeosciences Discuss. 2023, 1–28.

Slik, J., Eichhorn, K., 2003. Fire survival of lowland tropical rain forest trees in relation to stem diameter and topographic position. Oecologia 137, 446–455.

Stahl, A.T., Andrus, R., Hicke, J.A., Hudak, A.T., Bright, B.C., Meddens, A.J., 2023. Automated attribution of forest disturbance types from remote sensing data: A synthesis. Remote Sens. Environ. 285, 113416.

Tang, X., Bullock, E.L., Olofsson, P., Estel, S., Woodcock, C.E., 2019. Near real-time monitoring of tropical forest disturbance: New algorithms and assessment framework. Remote Sens. Environ. 224, 202–218.

Thompson, I.D., Guariguata, M.R., Okabe, K., Bahamondez, C., Nasi, R., Heymell, V., Sabogal, C., 2013. An operational framework for defining and monitoring forest degradation. Ecol. Soc. 18 (2).

UNFCCC, 2024. National inventory reports. 2024, (04-06-2024), URL https://unfccc.int/process-and-meetings/transparency-and-reporting/reporting-and-review/reporting-and-review-under-the-paris-agreement/national-inventory-reports.

Vancutsem, C., Achard, F., Pekel, J.-F., Vieilledent, G., Carboni, S., Simonetti, D., Gallego, J., Aragao, L.E., Nasi, R., 2021. Long-term (1990–2019) monitoring of forest cover changes in the humid tropics. Sci. Adv. 7 (10), eabe1603.

Viljur, M.-L., Abella, S.R., Adámek, M., Alencar, J.B.R., Barber, N.A., Beudert, B., Burkle, L.A., Cagnolo, L., Campos, B.R., Chao, A., et al., 2022. The effect of natural disturbances on forest biodiversity: an ecological synthesis. Biol. Rev. 97 (5), 1930–1947.

Wang, H., Ciais, P., Sitch, S., Green, J.K., Tao, S., Fu, Z., Albergel, C., Bastos, A., Wang, M., Fawcett, D., et al., 2024. Anthropogenic disturbance exacerbates resilience loss in the Amazon rainforests. Global Change Biol. 30 (1), e17006.

Weiskopf, S.R., Isbell, F., Arce-Plata, M.I., Di Marco, M., Harfoot, M., Johnson, J., Lerman, S.B., Miller, B.W., Morelli, T.L., Mori, A.S., et al., 2024. Biodiversity loss reduces global terrestrial carbon storage. Nat. Commun. 15 (1), 4354.

Wells, G.J., Ryan, C.M., Artur, L., Ribeiro, N., Bowers, S., Hargreaves, P., Fernando, J., Farao, A., Fisher, J.A., 2022. Tree harvesting is not the same as deforestation. Nat. Clim. Chang. 12 (4), 307–309.

Welsink, A.-J., Reiche, J., De Sy, V., Carter, S., Slagter, B., Suarez, D.R., Batros, B., Peña-Claros, M., Herold, M., 2023. Towards the use of satellite-based tropical forest disturbance alerts to assess selective logging intensities. Environ. Res. Lett. 18 (5), 054023.

Westman, W.E., Paris, J.F., 1987. Detecting forest structure and biomass with C-band multipolarization radar: Physical model and field tests. Remote Sens. Environ. 22 (2), 249–269.

van der Woude, S., Reiche, J., Sterck, F., Nabuurs, G.-J., Vos, M., Herold, M., 2024. Sensitivity of sentinel-1 backscatter to management-related disturbances in temperate forests. Remote. Sens. 16 (9), 1553.

Yanoviak, S.P., Gora, E.M., Bitzer, P.M., Burchfield, J.C., Muller-Landau, H.C., Detto, M., Paton, S., Hubbell, S.P., 2020. Lightning is a major cause of large tree mortality in a lowland neotropical forest. New Phytol. 225 (5), 1936–1944.

Zuleta, D., Arellano, G., McMahon, S.M., Aguilar, S., Bunyavejchewin, S., Castaño, N., Chang-Yang, C.-H., Duque, A., Mitre, D., Nasardin, M., et al., 2023. Damage to living trees contributes to almost half of the biomass losses in tropical forests. Global Change Biol. 29 (12), 3409–3420.